View Article Online / Journal Homepage / Table of Contents for this issue

J. CHEM. SOC. FARADAY TRANS., 1994, 90(24), 3693–3697

Samarium Oxide Catalyst; Formation, Characterization and Activity towards Propan-2-ol Decomposition

An IR Spectroscopic Study

Gamal A. M. Hussein
Chemistry Department, Faculty of Science, Minia University, El-Minia 61519, Egypt

IR spectroscopy has been used to study the gas-phase reaction products from the dehydrogenation–dehydration of propan-2-ol over Sm_2O_3 at temperatures between room temperature and 400 °C. Sm_2O_3 was shown to be a selective dehydration catalyst at 250 °C with decomposition of propan-2-ol to propene (*ca.* 90%). The Sm_2O_3 catalyst was obtained as a final decomposition product of $Sm(CH_3CO_2)_3 \cdot 4H_2O$. The thermal decomposition processes up to 800 °C were characterized by the thermogravimetry (TG), differential thermal analysis (DTA), X-ray diffraction (XRD) and IR spectroscopy. The compound dehydrates in two steps at 125 and 170 °C and recrystallizes at 195 °C. At 350 °C, the anhydrous acetate decomposes to $SmO(CH_3CO_2)$ *via* the intermediate $Sm(OH)(CH_3CO_2)_2$. At 450 °C two different phases of $Sm_2O_2(CO_3)$ are obtained which when further heated to 675 °C form Sm_2O_3. Surface area measurement and scanning electron microscopy showed that the final product, Sm_2O_3, at 800 °C has a surface area of 35 m^2 g^{-1} and is a crystalline porous material.

Published on 01 January 1994. Downloaded by Temple University on 30/10/2014 18:40:01.

IR spectroscopy has been used extensively to study the catalytic decomposition of alcohols over oxides of transition metals,[1] TiO_2, ZrO_2, HfO_2,[2–4] Al_2O_3 [5] and other oxides.[6,7] In contrast rare-earth-metal oxide catalysts have received little attention. The catalytic decomposition of alcohols, *via* dehydration and dehydrogenation is considered to be the main pathway for the production of materials of prime industrial importance.[8]

Samaria, with a fluorite structure, the final product of the decomposition of $Sm(CH_3CO_2)_3 \cdot 4H_2O$, has been used as a catalyst[9] and as a catalyst support for metals in the dehydration of alkan-2-ols to alk-1-enes and for metal oxides for the oxidative coupling of methane.[10,11] Sm_2O_3 is a basic metal oxide whose basicity and catalytic properties are dependent on the method of preparation and pretreatment.[10] It is well established[2–4,12] that the performance of solid catalysts and supports is largely dependent on the surface textural characteristics, which are determined by the preparation and pretreatment.[2,13,14]

High surface area metal oxide catalysts are often synthesized *via* the thermal decomposition of suitable precursor compounds.[14,15] The release of volatile components creates pores in the bulk.[16] An early study[17] of the thermal decomposition of $Sm(CH_3CO_2)_3 \cdot 1.5H_2O$ indicated that dehydration occurs at 150 °C, followed by decomposition at 700 °C to form Sm_2O_3 *via* a stable intermediate $Sm_2O_2CO_3$ at 450 °C.

In the present study the thermal decomposition of samarium acetate tetrahydrate was examined by TG and DTA. The gaseous products were identified by IR spectroscopy and the intermediate solid products by IR and XRD. The final decomposition product (Sm_2O_3) at 800 °C was examined by scanning electron microscopy and its surface area was determined. Its performance in the catalytic decomposition of propan-2-ol was studied.

Experimental

Materials

Samarium acetate tetrahydrate (SmAc) was 99.99% pure (Aldrich, USA). It was calcined at 250, 410 and 800 °C for 1 h in a static air atmosphere. The calcination temperatures were chosen on the basis of the thermal analysis results (see below). Propan-2-ol and acetone were spectroscopic grade products (BDH, UK). However, prior to use, they were thoroughly degassed by freeze–pump–thaw cycles performed under vacuum.

Thermal Analysis

TG and DTA of the parent material (SmAc), were carried out at different heating rates (θ = 2–20 °C min^{-1}) up to 800 °C, in a dynamic atmosphere of air (20 ml min^{-1}), using a model 30H Shimadzu analyser (Japan). 10–15 mg of the test sample was used for the TG measurements and highly sintered α-Al_2O_3 was the thermally inert reference material for the DTA.

IR Spectroscopy

IR spectra were obtained at a resolution of 5.3 cm^{-1}, over the frequency range 4000–400 cm^{-1}, using a model 580B Perkin-Elmer spectrophotometer equipped with a 3700 PE data station for spectra acquisition and handling. Gas-phase decomposition products were identified by means of IR spectra taken, after cooling to room temperature, from the atmosphere surrounding a 0.5 g portion of (SmAc) during heating at 10 °C min^{-1} to various temperatures (100–500 °C) for 5 min in a specially designed IR cell[18] equipped with KBr windows. The cell was evacuated briefly to 10^{-3} Torr prior to heating the sample.

IR spectra of SmAc and its calcination solid products were obtained from thin (>20 mg m^{-2}), lightly loaded (<1%) KBr-supported discs.

IR spectra of propan-2-ol and its catalytic decomposition gaseous products were taken in the same IR cell,[18] where the catalyst could be heated at various temperatures. The following standard procedure was adopted. The catalyst (100 mg in powder form) was heated in a stream of oxygen at 700 °C for 30 min to clean the surface of carbonate contamination[10] and then cooled to room temperature under vacuum (10^{-3} Torr). 10 Torr of the propan-2-ol vapour was admitted into the cell at various temperatures (100–400 °C), and maintained in contact with the catalyst for 10 min.

The amounts of propan-2-ol and the gaseous decomposition products were determined using the standard QUANT software of Perkin-Elmer and the on-line data acquisition system. The absorption intensity was measured at 3665 ± 5

View Article Online

Published on 01 January 1994. Downloaded by Temple University on 30/10/2014 18:40:01.

cm^{-1} for propan-2-ol, 1740 ± 5 cm^{-1} for acetone (the dehydrogenation product) and 910 ±5 cm^{-1} for propene (the dehydration product).[2]

XRD

XRD analysis of SmAc and its calcination products was carried out with a model JSX-60 PA Jeol diffractometer (Japan), equipped with a source of Ni-filtered Cu-Kα radiation. For identification purposes, diffraction patterns [I/I^0 *vs. d* spacing (Å)] obtained were matched with ASTM standards.

N_2 Adsorption

N_2 sorption isotherms were determined volumetrically at −196 °C using a micro-apparatus based on that described by Lippens *et al.*[19] The test sample (Sm_2O_3, 800 °C) was outgassed at 200 °C for 2 h under a vacuum of 10^{-5} Torr.

Electron Microscopy

A sample of the final decomposition product of SmAc at 800 °C was examined in a Jeol 35CF (Japan) scanning electron microscope. Before examination, the sample was rendered conducting by pre-coating with a thin film of Au–Pd.

Results and Discussion

TG and DTA curves recorded for SmAc heated to 800 °C at 20 °C min^{-1} are shown in Fig. 1. The curves indicate that SmAc decomposes *via* six endothermic weight loss (WL) processes, I, II, IV, V, VI and VII with maxima at 125, 170, 350, 375, 450 and 675 °C and one weight-invariant exothermic process, III, with a maximum at 195 °C. Fig. 2 shows IR gas-phase spectra, recorded over the frequency range 4000–500 cm^{-1}, of the atmosphere surrounding SmAc after heating at various temperatures for 5 min and then cooling to room temperature. IR spectra and X-ray powder diffractograms obtained for SmAc and its decomposition solid products at 250, 410 and 800 °C are shown in Fig. 3 and 4, respectively.

Fig. 5(*a*) shows the N_2-sorption isotherm for SmAc calcined at 800 °C for 1 h. The corresponding SEM is given in Fig. 5(*b*).

Fig. 6A shows the IR gas-phase spectra obtained after contacting 10 Torr of propan-2-ol with SmAc800 and heating consecutively for 10 min at the temperatures indicated. The composition of the gas-phase products is given in Fig. 6B.

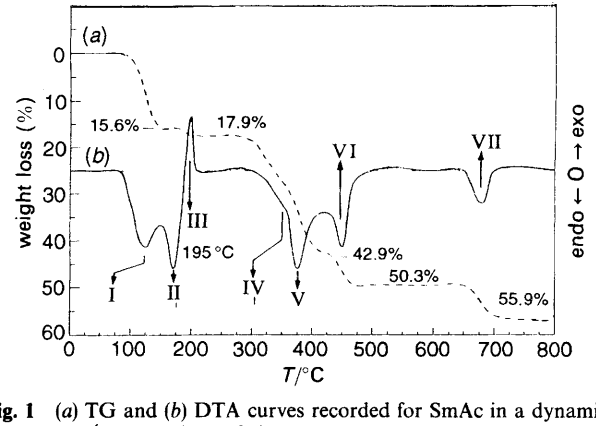

Fig. 1 (*a*) TG and (*b*) DTA curves recorded for SmAc in a dynamic (20 ml min^{-1}) atmosphere of air

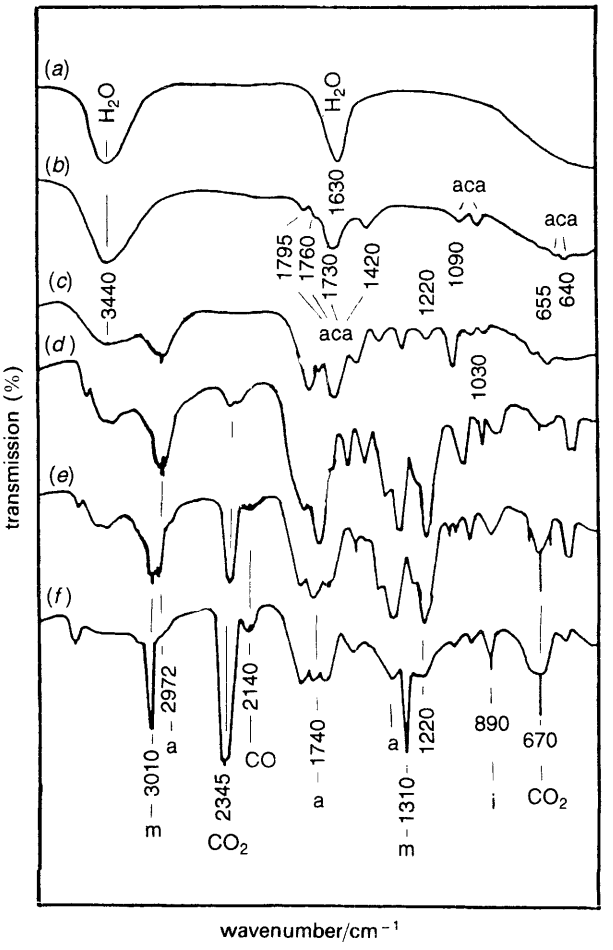

Fig. 2 IR spectra taken from the gas phase surrounding 0.5 g SmAc heated for 5 min at (*a*) 150, (*b*) 200, (*c*) 300, (*d*) 350, (*e*) 420 and (*f*) 500 °C; aca = acetic acid, a = acetone, m = methane and i = isobutene

Characterization of the Thermal Events

I *and* II (125–170 °C)

The IR spectra of the gaseous products at 150 and 200 °C show absorption bands at 3440 and 1630 cm^{-1} due to the ν(OH) and δ(HOH) vibrations, respectively, of the evolved water of crystallization.[20]

The WL determined for thermal events I and II (*ca.* 17.9%) (Fig. 1) is very close to the theoretical value (18.04%) expected for the release of four moles of H_2O, *i.e.*

$$Sm(CH_3O_2)_3 \cdot 4H_2O \xrightarrow[15.6\%]{\text{I(125 °C)}} Sm(CH_3O_2)_3 \cdot 0.5H_2O \xrightarrow[17.9\%]{\text{II(170 °C)}} Sm(CH_3O_2)_3 \quad (1)$$

III (195 °C)

Process III is weight-invariant and exothermic with a maximum at 195 °C (Fig. 1), *i.e.* immediately following the completion of the dehydration process II. The IR spectrum of the solid product at 250 °C (Fig. 3) is very similar to that of the unheated SmAc, with almost all the characteristic adsorption of acetate anions (at 1590–600 cm^{-1}).[20,21] However, there are two detectable differences: (*i*) absorption bands due to the $\nu_s(COO^-)$, $\nu_{as}(COO^-)$, ν(C—C) and $\delta(COO^-)$ at 1440, 1580, 965 and 460 cm^{-1}, respectively are shifted to lower frequencies in the product and (*ii*) the split absorption band at 1040 cm^{-1}, due to $\rho(CH_3)$ is shifted to lower frequencies and

View Article Online

Published on 01 January 1994. Downloaded by Temple University on 30/10/2014 18:40:01.

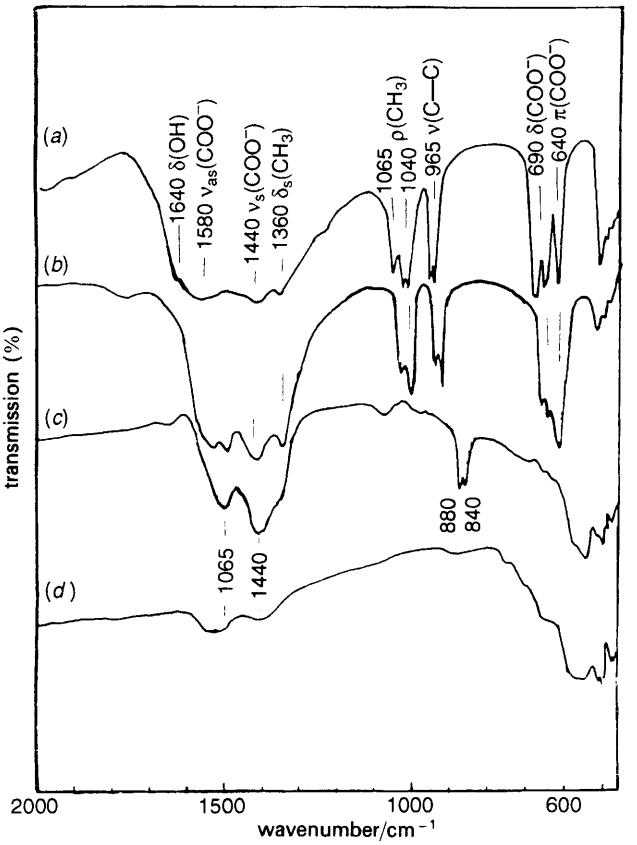

Fig. 3 IR spectra taken from KBr-supported samples of (*a*) SmAc and its decomposition solid products obtained by heating at (*b*) 250, (*c*) 410 and (*d*) 800 °C for 1 h

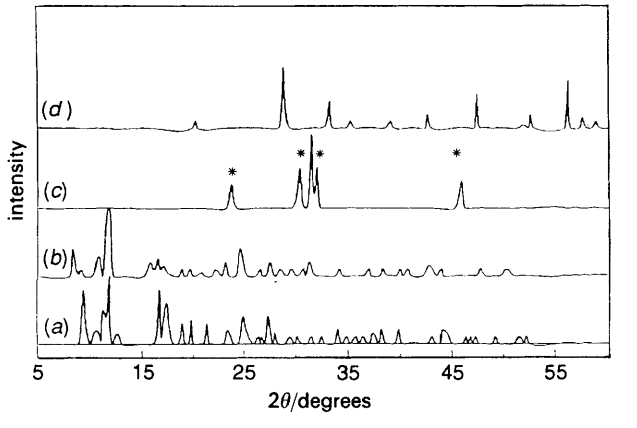

Fig. 4 X-Ray powder diffractograms of (*a*) SmAc and its decomposition products after heating at (*b*) 250 (*c*) 410 and (*d*) 800 °C for 1 h. (*a*) $Sm(CH_3CO_2)_3 \cdot 4H_2O$ (ASTM no. 27–572); (*b*) $Sm(CH_3CO_2)_3$ (ASTM no. 22–1300); (*c*) $Sm_2O_2CO_3$ (ASTM no. 23–625) and asterisked peaks $Sm_2O_2CO_3$(ASTM no. 37–806); (*d*) Sm_2O_3 (ASTM no. 5–813).

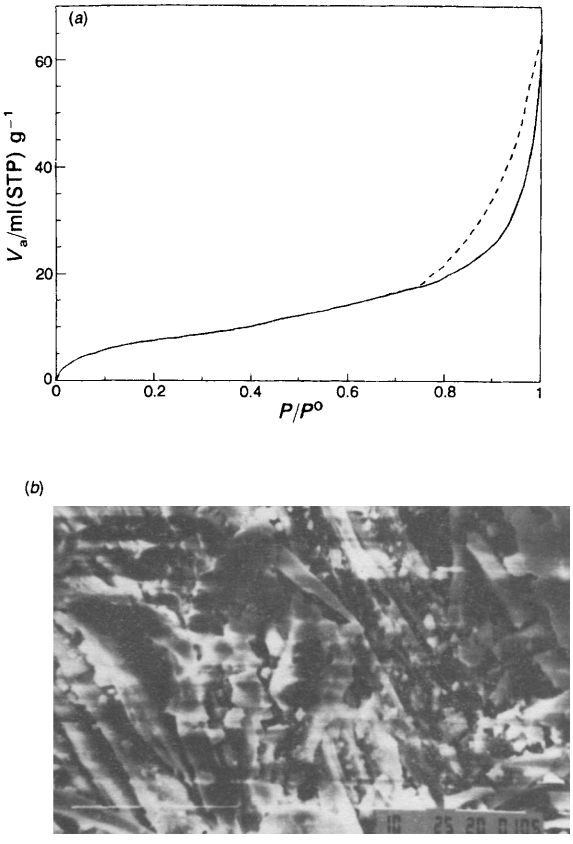

Fig. 5 (*a*) Nitrogen-sorption isotherm obtained for SmAc calcined at 800 °C, for 1 h at −196 °C using the BET method; (– – –) desorption, (——) adsorption. (*b*) SEM micrograph obtained (×7500) for SmAc calcined at 800 °C for 1 h.

the splitting disappears in the product spectrum. These modifications may suggest a restructuring of the acetate anions.[21,22] The corresponding XRD (Fig. 4) is consistent with that of anhydrous samarium acetate, ASTM no. 22–1300.

The IR gas-phase spectrum (Fig. 2) taken at 200 °C displayed weak absorptions at 1795, 1760, 1730, 1420, 1090 and 1030 cm^{-1}, due to acetic acid liberated as a result of the surface hydrolysis of acetate anions.[14,21,23] The low-frequency shifts experienced by the ν_{as} and ν_s vibrations of COO^-, shown in the IR spectrum of the solid-phase SmAc at 250 °C (Fig. 3) would indicate a weakening of the $Sm—OCOCH_3$ bonding.[22] Such a bond weakening, which may be induced as the water of dehydration is removed, seems to be responsible for making the surface acetates susceptible to hydrolysis.

IV *and* V (335–375 °C)

Processes IV and V (Fig. 1) are endothermic and overlap strongly. These two processes bring the total WL to 42.9% which is close to that expected (43.5%) for the formation of samarium oxyacetate, $SmO(CH_3CO_2)$. These results are in agreement with an earlier study[14] on the decomposition of $Pr(CH_3CO_2)_3 \cdot H_2O$), in which Pr oxyacetate was formed as an unstable intermediate.

The IR gas-phase spectra at 300 and 350 °C (Fig. 2), exhibit weakening of the absorptions due to water and reinforcement of the absorption bands characteristic of acetic acid vapour. Moreover, the bands due to acetone appear and are intensified at 350 °C. Thus, the formation of acetic acid at this stage, process IV, could be seen to occur *via* the possible intervention of ketene ($CH_2=C=O$)[24] as follows:

$$Sm(CH_3CO_2)_3(s) \rightarrow Sm(OH)(CH_3CO_2)_2(s) + CH_2=C=O(g) \quad (2)$$

$$CH_2=C=O(g) + H_2O(g) \rightarrow CH_3COOH(g) \quad (3)$$

However, the appearance of acetone in the gas phase is most probably due to the decomposition of the unstable intermediate $Sm(OH)(CH_3CO_2)_2$ and/or $Sm(CH_3CO_2)_3$ directly to

View Article Online

Published on 01 January 1994. Downloaded by Temple University on 30/10/2014 18:40:01.

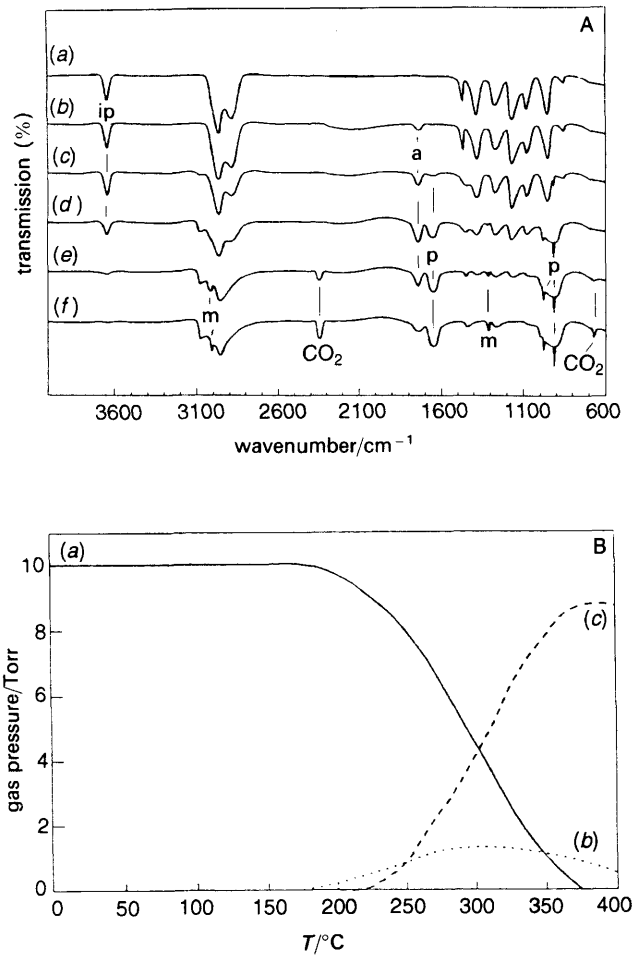

Fig. 6 A, IR spectra from 10 Torr propan-2-ol after contact with SmAc800 for 10 min at (*a*) 150, (*b*) 200, (*c*) 250, (*d*) 300 (*e*) 350 and (*f*) 400 °C. ip = propan-2-ol, a = acetone, p = propene, m = methanol. B, IR quantitative analysis of the gas-phase composition showing the relation between the reaction temperature and pressure (Torr), resulting from (*a*) and initial dose of 10 Torr propan-2-ol giving products of (*b*) acetone and (*c*) propene after consecutive 10 min intervals at the temperatures indicated over the catalyst SmAc800.

give $SmO(CH_3CO_2)$, through process V as follows:

$$Sm(CH_3CO_2)_3 \xrightarrow{IV} Sm(OH)(CH_3CO_2)_2(\text{unstable}) \xrightarrow{V} SmO(CH_3CO_2) \quad (4)$$

VI (450 °C)

Fig. 1 shows that the thermal process VI is endothermic and overlaps process V. The WL determined at the end of process VI, 50.3%, is close to that expected (50.7%) for the formation of $Sm_2O_2CO_3$, most probably by the following reaction:

$$2SmO(CH_3CO_2) \xrightarrow{VI} Sm_2O_2CO_3(s) + CH_3COCH_3(g) \quad (5)$$

In support of this mechanism, the IR gas-phase spectrum at 420 °C (Fig. 2) shows increased intensity of the absorption bands due to acetone. Moreover, the XRD of SmAc at 410 °C (Fig. 4) detects only $Sm_2O_2CO_3$ but in two different phases * $Sm_2O_2CO_3$ (ASTM no. 37–806) and $Sm_2O_2CO_3$ (ASTM no. 23–625). The IR spectrum of SmAc at 410 °C (Fig. 3) shows absorptions at 1560, 1440, 880 and 840 cm^{-1} assignable to oxycarbonate species.[25] The strong absorption appearing at 650–450 cm^{-1} are related to Sm—O vibrational modes.[25]

VII (675 °C)

On heating the sample further, process VII takes place endothermally (Fig. 1) at 675 °C. The maximum WL thus determined (55.9%) agrees well with the theoretical value (56.3%) expected for the overall conversion of SmAc to Sm_2O_3. Accordingly, the intermediate two phases of $Sm_2O_2CO_3$ must have decomposed to form Sm_2O_3.

The IR spectrum of SmAc at 800 °C (Fig. 3) shows no detectable absorptions due to oxycarbonate species. However, the absorptions below 850 cm^{-1}, related to lattice vibration modes of Sm_2O_3 remain.[25] The weak bands at around 1600, 1540 and 1440 cm^{-1} are most probably due to surface contamination by carbonate and moisture.[10] The corresponding XRD for SmAc at 800 °C (Fig. 4) shows only the pattern for crystalline Sm_2O_3 (ASTM No. 5–813).

Chemical Reactivity of the Gas/Solid Interface

The gas-phase IR spectra 420 and 500 °C (Fig. 2) also display bands due to methane (3010 and 1310 cm^{-1})[2,7,23] and isobutene (890 cm^{-1}).[2,7,23] Since the disappearance of acetone and the appearance of CH_4, CO_2 and isobutene occur over the same temperature range (400–500 °C), they are probably related. Moreover, the formation of both methane and isobutene is expected as a result of the involvement of acetone in surface-mediated bimolecular reactions.[2,26]

It has been shown earlier[2,7,14,15,26] that surface reactions of acetone over metal oxides can result in the formation of methane and isobutene:

$$(CH_3)_2CO(s) + OH^-(s) + (CH_3)_2CO(g) \rightarrow (CH_3)_2C{=}CH_2(g) + CH_3CO_2^-(s)$$

$$(CH_3)_2CO(g) + OH^-(s) \rightarrow CH_4(g) + CH_3CO_2^-(s)$$

(where s = surface and g = gas).

Surface Characterization

The N_2 adsorption isotherm at −196 °C, for SmAc calcined at 800 °C, is given in Fig. 5(*a*). The isotherm is similar to that of the type II isotherm in the BET classification,[27] indicative of a porous material. The hysteresis loop seen in Fig. 5(*a*) has nearly the shape of type (B) H3, This indicates that the majority of the pores are slit-shaped.[28] The closure point of the hysteresis loop is above $P/P^0 > 0.7$, this may indicate that the main pores are wide. However, the pore size analysis indicates both meso- and micro-porosity. The S_{BET} value determined for SmAc800 is 35 $m^2\ g^{-1}$. The SEM of the SmAc at 800 °C [Fig. 5(*b*)], supports the above results and reveals a wide size range of well formed crystals with rough surface steps and parallel cracks. The pores are randomly distributed over the surface with extensive porosity and are interplating shaped.

Catalytic Activity of Sm_2O_3 towards Propan-2-ol Decomposition

IR spectra taken from the gas-phase of propan-2-ol over Sm_2O_3 heated at different temperatures (150–400 °C) for 10 min are shown in Fig. 6A. The room temperature and 150 °C spectra display the characteristic bands of propan-2-ol.[2] At 200 °C a tiny but important absorption appears at 1740 cm^{-1}, which develops markedly in the 250 °C spectrum together with another absorption at 1250 cm^{-1}. The two bands mark the formation of acetone[2] vapour, and hence the dehydrogenation of propan-2-ol was seen to start at 200 °C. At 250 °C additional absorptions appear at 1650 (doublet) and 915 cm^{-1}. These absorptions are due to

View Article Online

propene. Hence the dehydration of propan-2-ol begins at 250 °C. At 300 °C, the spectrum shows a slight increase in acetone but a stronger increase in propene and the absorptions in the ν(CH) region (3100–2800 cm^{-1}) are restructured.

At 350 °C, the absorptions due to alcohol are hardly detectable and those due to acetone weaken. In contrast, the absorption due to propene is intensified. Moreover at 350 °C new absorptions appear at 3010 and 1310 cm^{-1} (due to methane)[2] and at 2340 and 670 cm^{-1} (due to CO_2).[23] These new absorptions are increased in the 400 °C spectrum. The formation of the byproducts CH_4 and CO_2, is due to surface reactions of acetone *via* an aldol-type condensation, involving adsorbed and gas-phase acetone molecules, as well as nucleophilic surface OH groups.

The above results are shown quantitatively, in Fig. 6B. It is clear that propan-2-ol starts to decompose at 200 °C, acetone appears simultaneously at 200 °C followed by propene at 250 °C. The rate of alcohol decomposition appears to be a maximum at 300 °C the production of propene (*ca.* 90%) at 350 °C and that of acetone (*ca.* 10%) at 300 °C. At 350 °C, the acetone concentration begins to decrease.

Conclusions

(1) SmAc decomposes completely at 675 °C to give Sm_2O_3 *via* the following pathways:

$$Sm(CH_3CO_2)_3 \cdot 4H_2O \xrightarrow{I} Sm(CH_3O_2)_3 \cdot 0.5H_2O \xrightarrow{II} Sm(CH_3CO_2)_3 \xrightarrow{III} Sm(CH_3O_2)_3 \text{ (crystallization)} \xrightarrow{IV} Sm(OH)(CH_3CO_2)_2 \xrightarrow{V} SmO(CH_2CO_2) \xrightarrow{VI} Sm_2O_2(CO_3) \text{ (two different phases)} \xrightarrow{VII} Sm_2O_3$$

(2) Evolution of acetic acid in the gas phase may be due to hydrolysis of ketene ($CH_2{=}C{=}O$) formed *via* the unstable intermediate $Sm(OH)(CH_3CO_2)_2$.

(3) Two different phases of $Sm_2O_2CO_3$ were detected as stable intermediates during the decomposition of SmAc.[14]

(4) Sm_2O_3 obtained at 800 °C has a surface area of 35 m^2 g^{-1} and exhibits both micro- and meso-porosity. (5) Sm_2O_3 obtained at 800 °C is a selective catalyst for the dehydration of propan-2-ol to propene (*ca.* 90%, at 350 °C), with dehydrogenation to acetone being only a maximum of *ca.* 10% at 300 °C.

References

1 J. Cunningham, B. K. Hodnett, M. Ilyas, J. Tobin and E. L. Leahy, *Discuss. Faraday Soc.*, 1981, **72**, 283.
2 G. A. M. Hussein, N. Sheppard, M. I. Zaki and R. B. Fahim, *J. Chem. Soc., Faraday Trans. 1*, 1989, **85**, 1723.
3 G. A. M. Hussein, N. Sheppard, M. I. Zaki and R. B. Fahim, *J. Chem. Soc., Faraday Trans.*, 1991, **87**, 2655.
4 G. A. M. Hussein, N. Sheppard, M. I. Zaki and R. B. Fahim, *J. Chem. Soc., Faraday Trans.*, 1991, **87**, 2261.
5 H. Knozinger and W. Stuhlin, *Progr. Colloid Polym. Sci.*, 1980, **67**, 33.
6 O. V. Krylov, *Catalysis by Non-Metals*, Academic Press, New York, 1970, pp. 115.
7 M. I. Zaki and N. Sheppard, *J. Catal.*, 1983, **80**, 114.
8 I. Wender, *Catal. Rev.*, 1984, **26**, 304.
9 K. Thomke, *Z. Phys. Chem.*, 1977, **106**, 225.
10 K. Tanabe, K. Mismo, Y. Ono and H. Hattori, *New Solid Acids and Bases*, Kodansha, Tokyo, 1989, pp. 41–47.
11 H. Arakawa, *Techno Japan*, 1988 **21**, 32.
12 F. Morelli, M. Giorgini and R. Tartarelli, *J. Catal.*, 1972, **26**, 106.
13 D. L. Trim and A. Stanislaus, *Appl. Catal.*, 1986, **21**, 215.
14 G. A. M. Hussein, *J. Anal. Appl. Pryolysis*, 1994, **29**, 89.
15 S. A. A. Mansour, G. A. M. Hussein and M. I. Zaki, *Thermochim. Acta*, 1989, **150**, 153.
16 S. A. A. Mansour, M. A. Mohamed and M. I. Zaki, *Thermochim. Acta*, 1988, **129**, 189.
17 R. C. Paul, M. S. Bains and J. S. Ghotra, *Indian J. Chem.*, 1964, **7**, 514.
18 J. B. Peri and B. H. Hannan, *J. Phys. Chem.*, 1960, **64**, 1526.
19 B. C. Lippens, B. G. Linsen and J. H. de-Boer, *J. Catal.*, 1964, **3**, 32.
20 K. Nakamoto, *Infrared Spectra of Inorganic and Coordination Compounds*, Wiley, New York, 1970, pp. 253.
21 G. A. M. Hussain, *J. Thermal Anal.*, 1994, **41**, in the press.
22 D. M. Griffiths and C. H. Rochester, *J. Chem. Soc., Faraday Trans. 1*, 1987, **74**, 403.
23 R. H. Pierson, A. M. Fletcher and E. St. Clair Gantz, *Anal. Chem.*, 1956, **28**, 1218.
24 A. K. Galwey and M. A. Mohamed, *J. Chem. Soc., Faraday Trans. 1*, 1985, **81**, 2503.
25 J. A. Goldsmith and S. D. Ross, *Spectrochim. Acta, Part A*, 1967, **23**, 1909.
26 G. A. M. Hussein, *Thermochim. Acta*, 1991, **180**, 187.
27 S. J. Gregg and K. S. W. Sing, *Adsorption, Surface Area and Porosity*, Academic Press, London, 2nd edn., 1982.
28 K. S. W. Sing, *Pure Appl. Chem.*, 1982, **54**, 2201.

Paper 4/04559I; *Received* 25*th July*, 1994

Published on 01 January 1994. Downloaded by Temple University on 30/10/2014 18:40:01.